Properties and chemical stability of hotrolled Ag(7 at.% Cu)sheathed Bi2Sr2Ca0.64Cu1.64O x powderintube tapes

J. Guo, J. A. Lewis, K. C. Goretta, and J. Schwartz

Citation: Journal of Applied Physics **78**, 4596 (1995); doi: 10.1063/1.359805
View online: http://dx.doi.org/10.1063/1.359805
View Table of Contents: http://scitation.aip.org/content/aip/journal/jap/78/7?ver=pdfcov
Published by the AIP Publishing

Properties and chemical stability of hot-rolled Ag(7 at. % Cu)-sheathed $Bi_2Sr_2Ca_{0.64}Cu_{1.64}O_x$ powder-in-tube tapes

J. Guo
Department of Materials Science and Engineering, University of Illinois, Urbana, Illinois 61801

J. A. Lewis[a)]
Department of Materials Science and Engineering, NSF Science and Technology Center for Superconductivity, University of Illinois, Urbana, Illinois 61801

K. C. Goretta
Energy Technology Division, Argonne National Laboratory, Argonne, Illinois 60439

J. Schwartz
National High Magnetic Field Laboratory, Florida State University, Tallahassee, Florida 32316; Department of Mechanical Engineering, FAMU/FSU College of Engineering, Florida State University, Tallahassee, Florida 32316

(Received 31 March 1995; accepted for publication 26 June 1995)

$Bi_2Sr_2Ca_{0.64}Cu_{1.64}O_x$ (nominally Bi2212) powders were fabricated into powder-in-tube Ag- and Ag(7 at. % Cu)-sheathed tapes by cold and hot rolling to investigate the effects of sheath composition and rolling conditions on their microstructural development and superconducting properties. Bi2212 tapes with Ag(Cu) sheaths exhibited improved grain alignment and interfacial uniformity, as well as enhanced formation of the Bi-free phase ($\approx Sr_{7.5}Ca_{6.5}Cu_{14}O_x$), relative to the Ag-sheathed specimens. The hot-rolled Ag(Cu)-sheathed tapes displayed superior critical current densities (J_c), where magnetization $J_{cm}=1.5\times10^6$ ($H\|c$) and 4.6×10^5 A/cm^2 ($H\perp c$) at $T=5$ K, $H=1$ T. Correspondingly, these specimens had transport critical current densities (J_{ct}) of 6.7×10^4 A/cm^2 ($H\|c$) and 5.4×10^4 A/cm^2 ($H\perp c$) at $T=4.2$ K, $H=0$ T and 2.2×10^4 A/cm^2 ($H\|c$) and 3.0×10^4 A/cm^2 ($H\perp c$) at $T=4.2$ K, $H=14$ T. The chemical stability of the Ag(Cu) sheath regions during the partial melting process was also studied. Rapid oxidation of copper produced Cu_2O precipitates in the sheath at 885 °C, and subsequently a Cu_2O-free zone developed near the core/sheath interface. A theoretical analysis of Cu_2O precipitate formation and decomposition during thermal processing is presented. © *1995 American Institute of Physics.*

I. INTRODUCTION

$Bi_2Sr_2Ca_1Cu_2O_{8+x}$ (Bi2212) is a promising high-T_c superconducting material for large-scale applications due to its ease of fabrication via the powder-in-tube (PIT) method and its ability to transport large current densities ($>10^4$ A/cm^2) in high magnetic fields at temperatures above 4.2 K. Because of its highly anisotropic nature, previous research efforts have focused on improving Bi2212 grain alignment in PIT tapes.[1–4] We have demonstrated that improved grain alignment and critical current carrying capability can be achieved by hot rolling Ag-sheathed Bi(2212) PIT tapes.[5,6] Perin *et al.*[7] reported similar improvements in hot-rolled Ag-sheathed $Bi_2Sr_2Ca_2Cu_3O_{10+x}$ (Bi2223) tapes. However, this approach produces irregularities at the metal sheath/oxide core interface due to increased mechanical-property differences between these regions at elevated temperatures. To minimize such differences, stiffer sheath materials such as cold-worked Ag(Cu) alloys have been recently proposed by other investigators.[8] Here, we study the effects of rolling conditions and sheath composition on the microstructural development, chemical stability, and superconducting properties of Ag(7 at. % Cu)-sheathed Bi2212 PIT tapes.

[a)]Electronic mail: jalewis@ux1.cso.uiuc.edu

II. EXPERIMENTAL PROCEDURE

Ag- and Ag(7 at. % Cu)-sheathed Bi2212 tapes were prepared by the conventional powder-in-tube procedure.[1–6] $Bi_2Sr_2Ca_{0.64}Cu_{1.64}O_x$ powder was packed into pure Ag and Ag(7 at. % Cu) tubes, drawn into wires, cold-rolled into tapes with thicknesses of 0.3 mm, and then partially melted. The thermal schedule for partial melting is shown in Fig. 1. Differential thermal analysis (DTA) was used to study the melting behavior of the sheath materials in the presence and absence of the superconducting cores. The samples were heated at 5 °C/min in air to a maximum temperature of 950 °C.

To investigate the chemical stability of the Ag(Cu) alloy sheaths during thermal treatment, Ag(Cu)-sheathed PIT tapes were inserted into a preheated furnace and heated under isothermal conditions in stagnant air for various times, where $T_{iso}=820$ or 885 °C. The samples were then quenched in air by withdrawing them directly from the furnace.

Hot rolling ($T_{roll}=420$ °C) was carried out on partially melted Ag(7 at. % Cu)-sheathed tapes preheated to 800 °C in air for 2 min prior to each pass. The surfaces of the hot rolls were coated with a thin layer of boron nitride to ensure smooth tape surfaces and to prevent the samples from adhering to the rolls. For comparison, representative Ag- and Ag(7 at. % Cu)-sheathed tapes were also rolled using cold rolls ($T_{roll}\approx22$ °C). During each rolling pass, the tape thickness

 0021-8979/95/78(7)/4596/12/$6.00

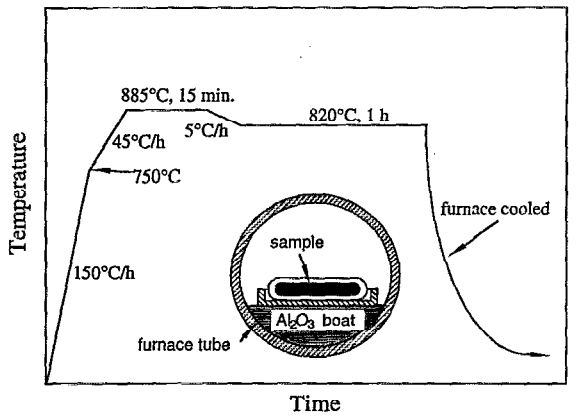

FIG. 1. Partial-melting schedule used during heat treatment of Bi2212 PIT tapes. (Inset is schematic view of sample placement in furnace.)

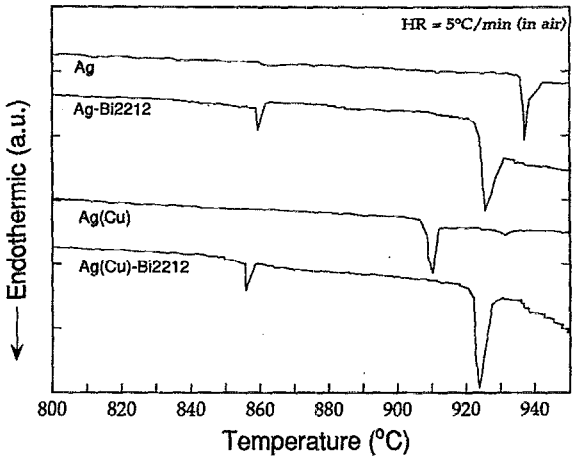

FIG. 2. Differential thermal analysis curves for pure Ag sheath, Ag-sheathed Bi2212 tape, pure Ag(Cu) sheath, and Ag(Cu)-sheathed Bi2212 tape heated at 5 °C/min in air.

was reduced by approximately 10%. After six passes, the resulting tapes were annealed at 800 °C for 100 h in stagnant air.

The broad surface and longitudinal cross sections of representative isothermally heated, partially melted, and partially melted, rolled Ag- and Ag(Cu)-sheathed tapes were polished and examined by optical microscopy, x-ray diffraction (XRD), and scanning electron microscopy (SEM). CuK_α radiation was used for XRD with a voltage of 40 kV and a current of 20 mA. A Hitachi S-800 SEM equipped with a Link energy-dispersive spectrometer (EDS) was used to examine the grain composition and alignment, as well as the interfacial uniformity of these samples. The cold- and hot-rolled specimens were etched for 60 s with a solution of two parts perchloric acid mixed with 98 parts 2-butoxyethanol prior to SEM analysis. This procedure led to enhanced microstructural features and was necessary due to the higher core densities of these samples relative to the partially melted tapes. A Leitz Wetzlar monoload hardness tester was used to measure the microhardness of each sheath material after hot rolling. These measurements were obtained on the transverse cross section of each specimen.

The superconducting properties of cold- and hot-rolled PIT tapes were measured in a Quantum Design dc superconducting quantum interference device (SQUID). Magnetic hysteresis measurements were made in applied magnetic fields of ± 7.0 T at temperatures between 5 and 25 K. Samples were oriented either parallel ($H \| c$) or perpendicular ($H \perp c$) to the applied field, given the approximate c-axis grain alignment perpendicular to the sample surface. Critical current densities, J_{cm} were estimated with the Bean model,[9] $J_{cm} = 30\ \Delta M/d$, where d is the width of the oxide core, as determined by SEM analysis. Transport current densities, J_{ct}, were measured at $T = 4.2$ K in an applied field ($H = 0 - 17$ T) by the four-probe resistivity technique with sample length of 2 cm. An electric field criterion of 1 μv/cm was used to ascertain the critical current for the voltage–current measurements.

III. RESULTS

A. Microstructural characterization

1. Phase analysis

The DTA results obtained for pure Ag- and Ag(Cu)-sheathed materials and Ag- and Ag(Cu)-sheathed tapes are shown in Fig. 2. In the presence of the oxide core, the silver sheath melts at approximately 924 °C, compared to 934 °C for the pure silver in air. In the Ag-sheathed tapes, the oxide core undergoes peritectic decomposition at 859 °C, which is significantly lower than for pure Bi2212 powder, which decomposes between 875 and 890 °C in air. In comparison, the Ag(Cu) sheath material melts at 904 °C (≈30° lower than the silver sheath). However, in the presence of an oxide core, the melting point of the Ag(Cu) sheath is elevated to 924 °C. This temperature is equivalent to that observed for the Ag sheath material in the presence of the oxide core. In the Ag(Cu)-sheathed tapes, the oxide core undergoes peritectic decomposition at 858 °C.

Figure 3 depicts a series of SEM micrographs of the polished longitudinal cross sections of partially melted, cold-rolled, and hot-rolled Ag- and Ag(Cu)-sheathed PIT tapes, where Fig. 3(e) corresponds to a hot-rolled Ag-sheathed Bi2212 tape of a similar nominal composition (from Ref. 5). The nonetched, partially melted tapes, shown in Figs. 3(a) and 3(b), have core and sheath thicknesses of approximately 120 and 70 μm, respectively. The partially-melted Ag-sheathed tape has a much lower density relative to the Ag(Cu)-sheathed tape, containing several large voids within the core region. Upon cold or hot rolling (≈60% total deformation), the core thicknesses of the Ag- and Ag(Cu)-sheathed tapes were reduced to approximately 50 μm, as shown in Figs. 3(c)–3(f). The as-rolled tapes were etched prior to SEM analysis, as discussed previously. This procedure appears to preferentially remove nonsuperconducting phases, allowing for improved visualization of the Bi2212 grain structure within the core regions. One artifact of this

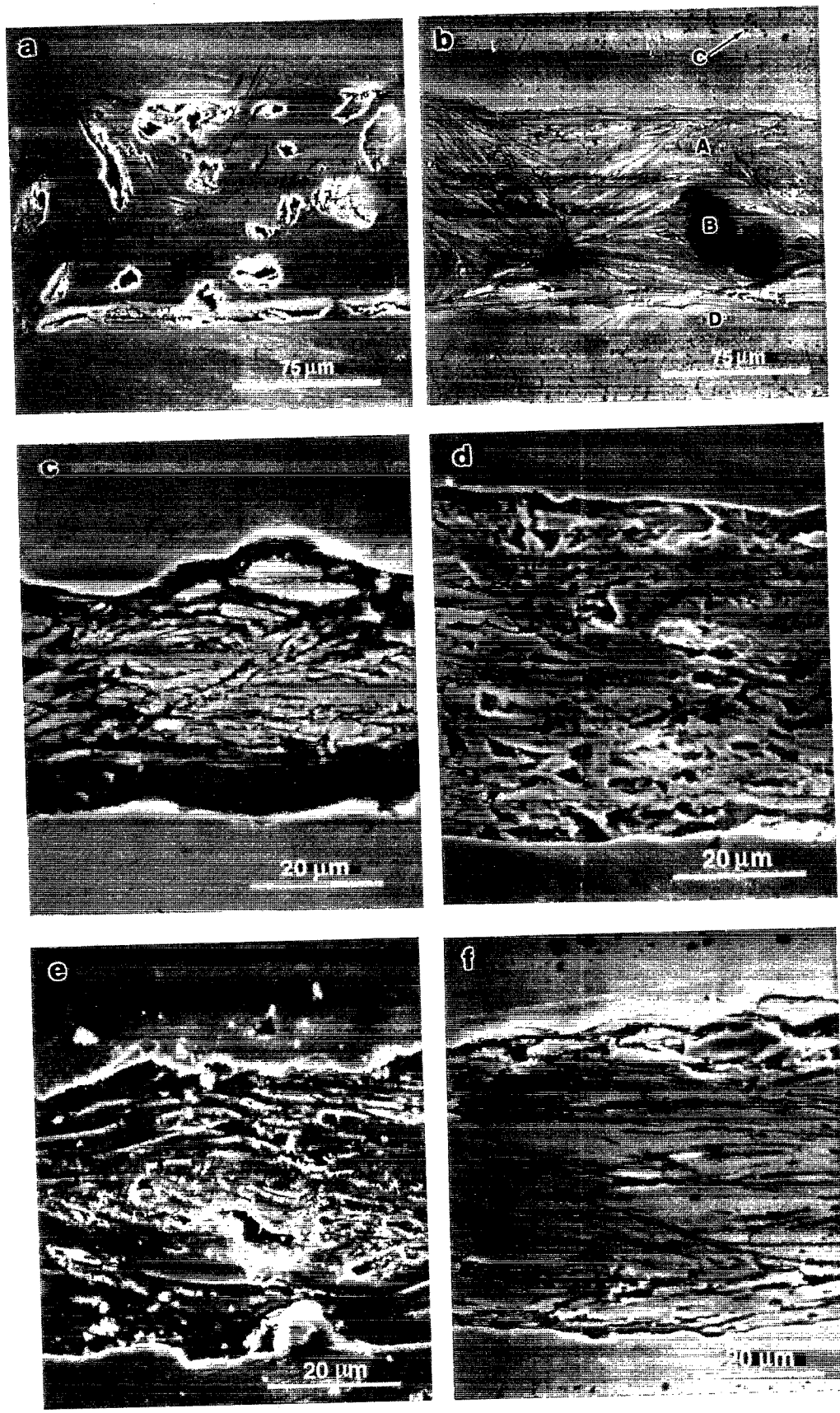

FIG. 3. SEM photomicrographs of longitudinal cross sections of Bi2212 core within (a) partially melted, Ag-sheathed tape, (b) partially melted, Ag(Cu)-sheathed tape, (c) cold-rolled, Ag-sheathed tape, (d) cold-rolled, Ag(Cu)-sheathed tape, (e) hot-rolled, Ag-sheathed tape, and (f) hot-rolled, Ag(Cu)-sheathed tape. [Note: (e) was reproduced from Ref. 5.]

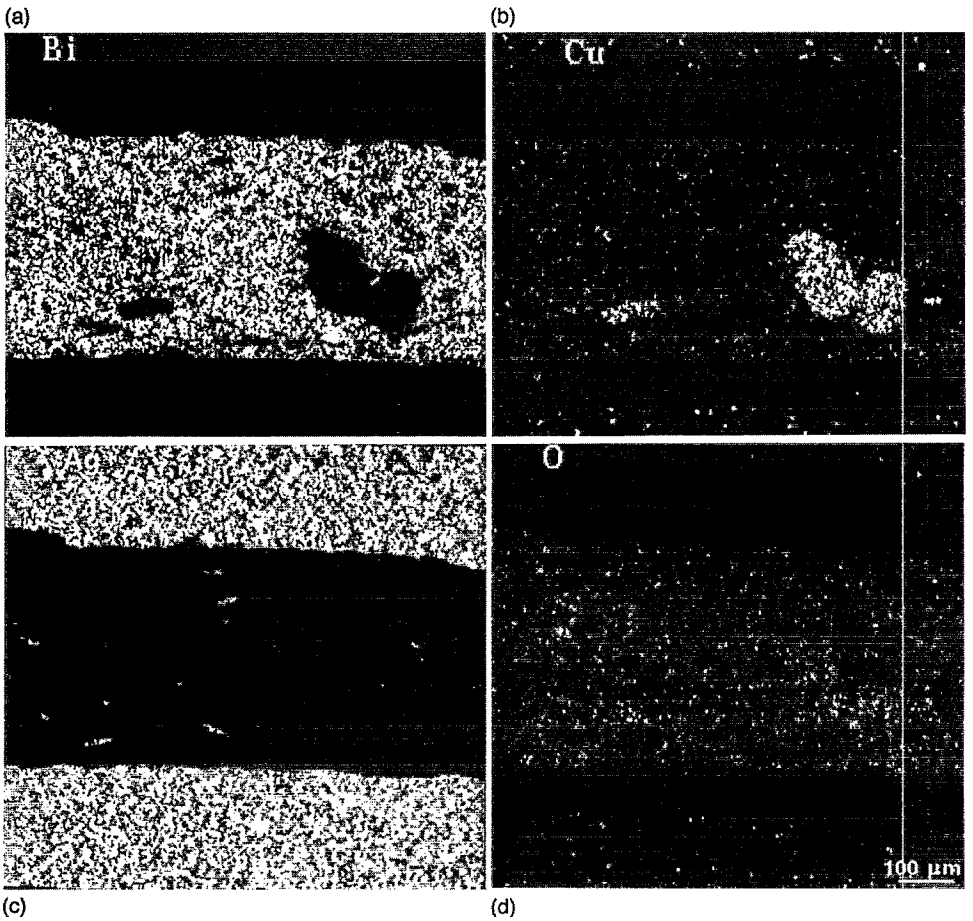

FIG. 4. Element distribution maps of area shown in Fig. 3(b) for (a) bismuth, (b) copper, (c) silver, and (d) oxygen.

process, however, is the delaminated appearance of these samples relative to the nonetched, partially melted specimens.

The formation of secondary phases during partial melting was more pronounced in the Ag(Cu)-sheathed tapes, as shown in Figs. 3(a) and 3(b). Element distribution maps of the same microstructural area shown in Fig. 3(b) are given in Fig. 4 for bismuth, copper, silver, and oxygen. The dark core regions in Fig. 3(b) correspond to the alkaline-earth cuprate phase, which is both Cu-rich and Bi-free (see Fig. 4). Quantitative EDS analysis of these regions indicates that the approximate composition of this alkaline-earth cuprate phase is $Sr_{7.5}Ca_{6.5}Cu_{14}O_x$, as shown in Fig. 5. Because the Ag- and Ag(Cu)-sheathed tapes each consist of the same starting oxide composition, it appears that the copper-containing sheath material promotes the formation of the unwanted Bi-free alkaline-earth cuprate phase. Previously, we have shown that the amount of Bi-free phase(s) in the Ag-sheathed tapes were reduced in both size and volume fraction after rolling and final heat treatment.[5,6] SEM and optical microscopy confirm this trend in the present work for the Ag-sheathed specimens. In contrast, there is less reduction of the Bi-free phase in Ag(Cu)-sheathed tapes after rolling and final heat treatment.

The copper and oxygen elemental maps shown in Fig. 4 also reveal the presence of Cu- and oxygen-rich regions in the sheath region. These regions correspond to black precipitates in the Ag(Cu) sheaths shown in Fig. 3(b). Quantitative EDS analysis of these regions is shown in Fig. 5. Analysis of CuO and Cu_2O standards indicated that these precipitates were Cu_2O. A distinct Cu_2O-deficient zone approximately 25–30 μm wide was observed in the Ag(Cu) sheath near the sheath/core interface in the Ag(Cu)-sheathed PIT tapes.

To further understand the morphological development that occurs in the Ag(Cu)-sheaths in these partially melted PIT tapes, a series of isothermal quench studies were carried out. Two hold temperatures were used, corresponding to the maximum temperature (T_{max}) of 885 °C and the soak temperature (T_{soak}) of 820 °C experienced during partial melting. SEM photomicrographs of the longitudinal, polished cross sections of the Ag(Cu)-sheathed tapes heated at 820 and 885 °C for various times are shown in Figs. 6 and 7, respectively. Cu_2O precipitates formed rapidly near the outer sheath surface and the sheath/core interface at both temperatures. As time progressed, the Cu_2O precipitate-filled regions grew inward toward the center of the sheath. At relatively short times of roughly 400 s at T_{iso}=820 °C and 200 s at T_{iso}=885 °C, the Cu_2O precipitates were observed throughout the sheath cross sections, as shown in Figs. 6(b) and 7(b), respectively. Upon extended annealing at these temperatures (i.e., 12 h at 820 °C and 6 h at 885 °C), Cu_2O-deficient zones were observed near the sheath-core interfaces, as shown in Figs. 6(c) and 7(c), respectively. These photomicrographs

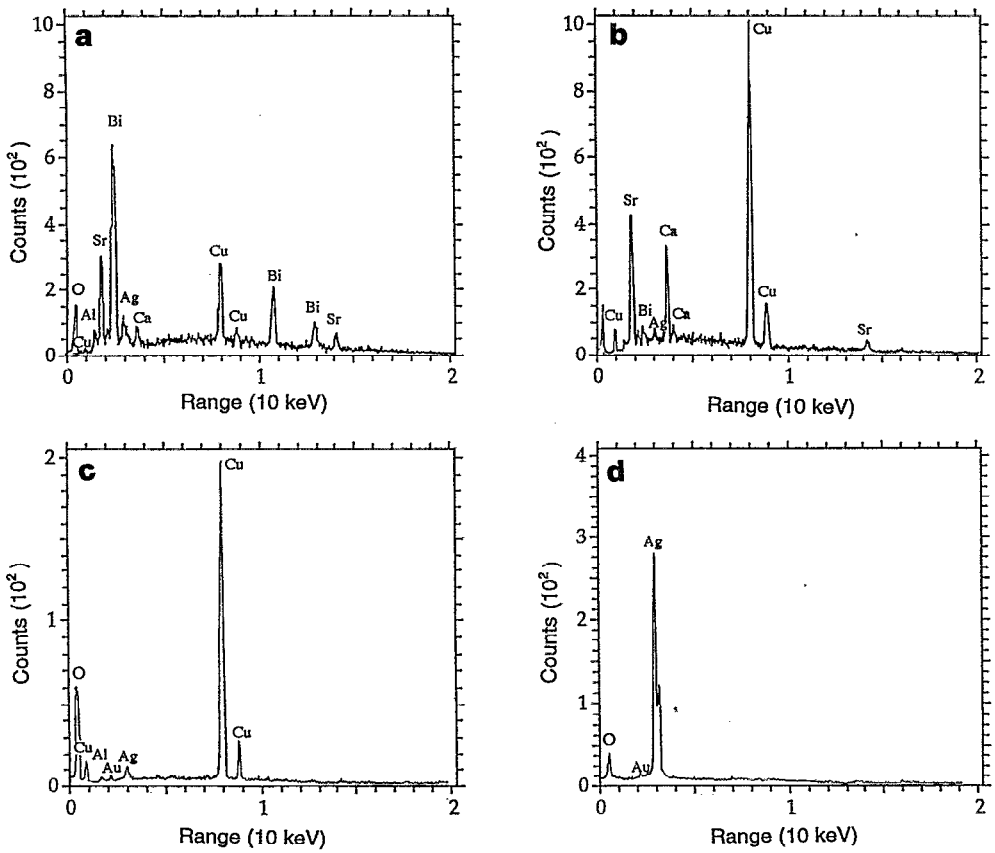

FIG. 5. EDXS compositional analyses of regions indicated in Fig. 3(b): (Area A) Bi2212 phase, (Area B) Bi-poor phase, (Area C) Cu_2O precipitates, and (Area D) Cu-free zone.

correlate well to the final sheath microstructures observed in the partially melted Bi2212 Ag(Cu)-sheathed tapes studied here, as well as to those reported previously by Nomura *et al.*[8] for doctor blade Bi2212 tapes (thickness ≈20 μm) heat treated on Ag(2.6 at. % Cu) foil (thickness ≈50 μm). The earlier work of Nomura and co-workers,[8] however, neglected to fully explore the interactions between Bi2212 and Ag(Cu) alloy materials. A theoretical analysis of the chemical stability of the Ag(Cu) sheaths during partial melting will be discussed later.

2. Grain alignment

Well-aligned Bi2212 cores were obtained in the hot-rolled Ag(Cu)-sheathed tapes (see Fig. 3). As an example,

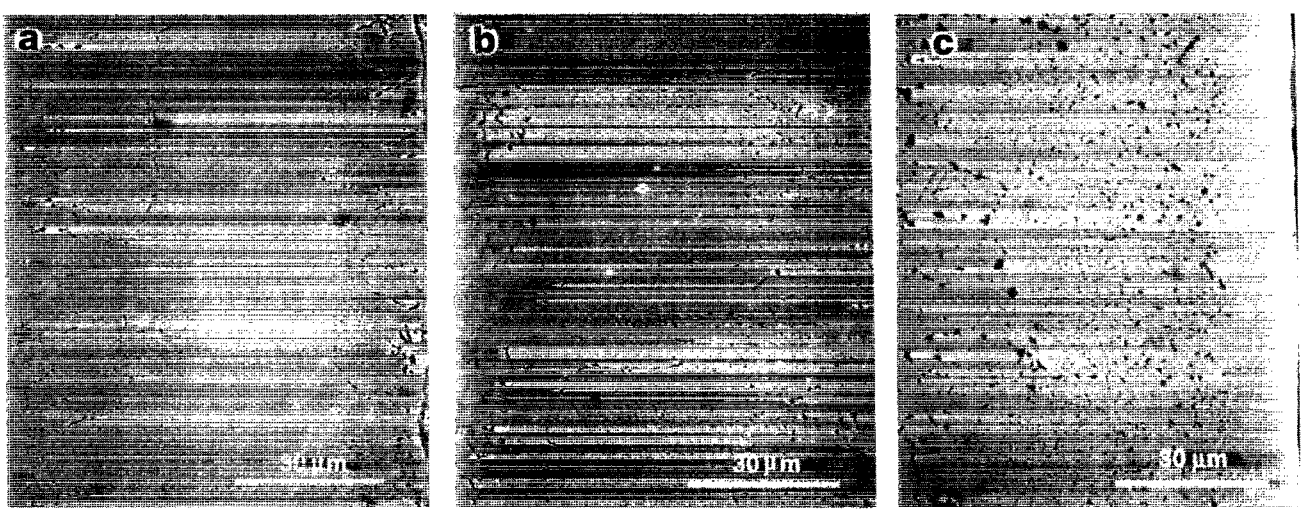

FIG. 6. SEM photomicrographs of longitudinal cross sections of Ag(Cu) sheath regions of Bi2212 tapes fired at 820 °C in air for: (a) 200 s, (b) 400 s, and (c) 12 h.

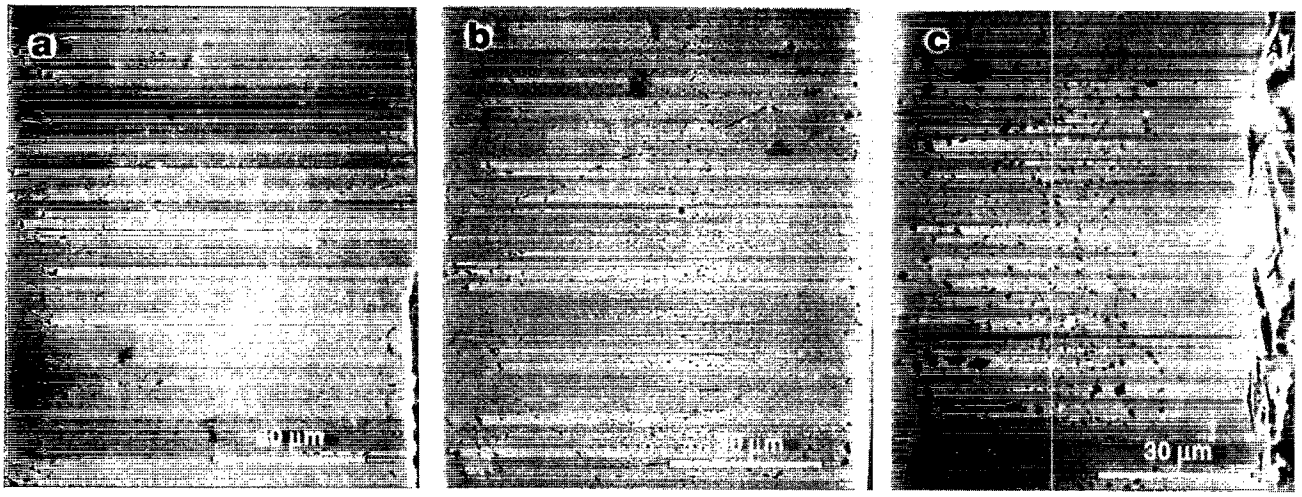

FIG. 7. SEM photomicrographs of longitudinal cross sections of Ag(Cu) sheath regions of Bi2212 tapes fired at 885 °C in air for (a) 100 s, (b) 200 s, and (c) 6 h.

textured grains roughly 60–80 μm in length were observed in the Ag(Cu)-sheathed specimen hot rolled at 420 °C and then annealed at 800 °C for 100 h [Fig. 3(f)]. XRD patterns obtained from the polished tape surfaces are shown in Fig. 8. The degree of grain alignment was quantified by the ratio (R) of the relative intensities of two major peaks, as given by $R=I_{(0010)}/(I_{(117)}+I_{(0010)})$. Consistent with the SEM observations, the hot-rolled Ag(Cu)-sheathed tapes exhibited the highest degree ($R=0.96$) of c-axis texture, as shown in Fig. 9. Major improvements in grain alignment occurred during the first stages of the hot-rolling process, where less than 50% of the total deformation occurred. Hot rolling, combined with preheating the PIT tapes, is believed to facilitate Bi2212 grain rearrangement by promoting liquid phase formation.[6] The extent of liquid phase formation can be controlled by adjusting the preheating temperature to induce melting of the Bi2212 phase,[10–16] or by incorporating low melting additives.[17–22]

3. Sheath/core interface uniformity

As reported previously for Bi2212 tapes of similar nominal composition,[5,6] hot rolling causes enhanced irregularities at Ag sheath–oxide core interfaces due to mechanical property differences between these materials, and these differences are exacerbated at elevated temperatures. The longitudinal (see Fig. 3) and transverse cross sections of the PIT tapes reveal that, in addition to better grain alignment, the sheath/oxide interfaces were significantly improved in the Ag(Cu)-sheathed tapes relative to the pure Ag-sheathed tapes. We attribute this to the measured hardness differences between the Ag(Cu)- and Ag-sheath materials, as shown in Fig. 10. For example, the hardness of the as-rolled Ag(Cu) material was roughly 43% (at 0% reduction) and 27% (after 30% total reduction) greater than that observed for pure silver. These values are significant because the majority of core densification and grain rearrangement occurs during this stage of the rolling process.

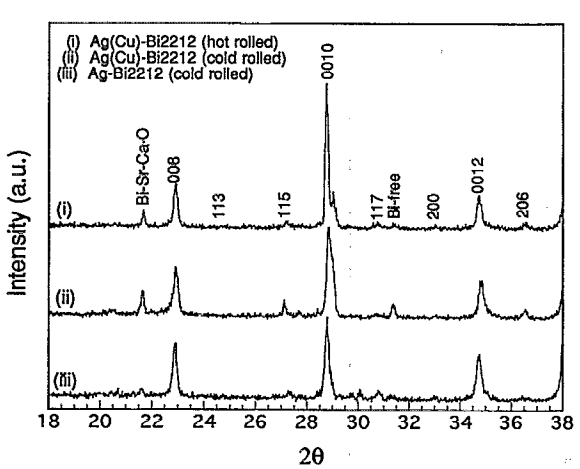

FIG. 8. XRD patterns of final cold- and hot-rolled Bi2212 tapes.

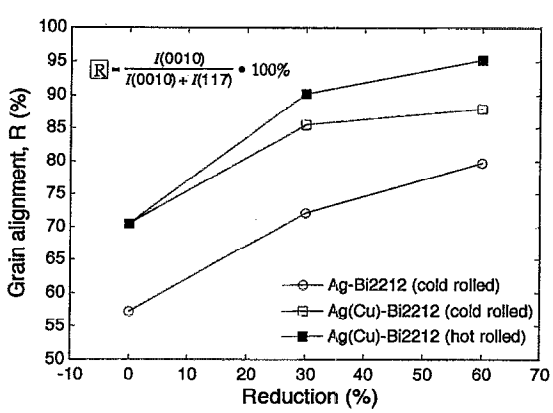

FIG. 9. Plot of grain alignment as a function of rolling reduction for cold- and hot-rolled Bi2212 tapes.

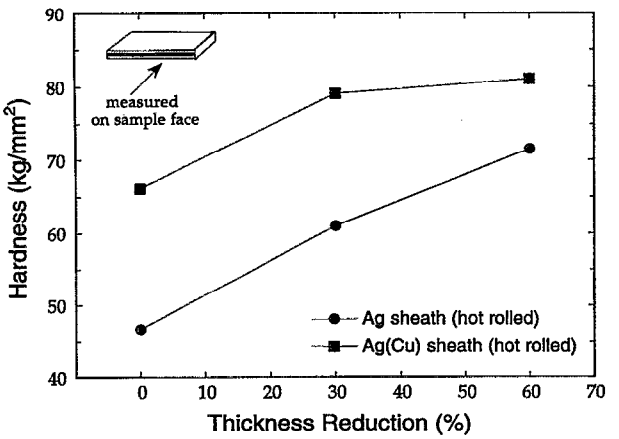

FIG. 10. Plot of sheath hardness as a function of rolling reduction for hot-rolled Ag- and Ag(Cu)-sheathed Bi2212 tapes. (Arrow indicates area sampled during these measurements.)

B. Superconducting properties

1. Magnetization J_{cm}

Figure 11 shows the width of the magnetization hysteresis curves, ΔM, and the corresponding Bean critical current densities, J_{cm}, for the as-rolled Ag(Cu)-sheathed Bi2212 tapes as a function of applied field for several temperatures. As stated previously, the J_{cm} values are derived assuming a constant value of d equivalent to the core width of each sample. $J_{cm}(H\|c)$ dropped more sharply with temperature than $J_{cm}(H\perp c)$ in both the cold- and hot-rolled specimens. Notably, the J_{cm} for the hot-rolled Ag(Cu)-sheathed tapes is three to four times higher than that of cold-rolled Ag(Cu) tapes, and a factor of almost 10 higher than the hot-rolled Ag-sheathed tape (see Ref. 5), as shown in Fig. 12 ($T=5$ K). Interestingly, however, the J_{cm} for the 800 °C preheated Ag(Cu) tape rolled through room-temperature rolls is even lower than that of cold-rolled tape, as shown in Fig. 12.

2. Transport J_{ct}

The transport critical current density, J_{ct}, as a function of applied field for a representative section of the hot-rolled Ag(Cu)-sheathed tape oriented $H\|c$ and $H\perp c$ is shown in Fig. 13. These values revealed some hysteresis with respect to the field increasing and decreasing measurements. J_{ct} values above 2×10^4 A/cm^2 ($H\|c$) and 3×10^4 A/cm^2 ($H\perp c$) at 4.2 K were obtained in magnetic fields up to 14 T. Furthermore, the J_{ct} value (6.7×10^4 A/cm^2) for this specimen at 4.2 K in zero field is roughly five times greater than that of the hot-rolled Ag-sheathed tape (1.25×10^4 A/cm^2) reported previously.[5] However, the transport J_{ct} is about one order of

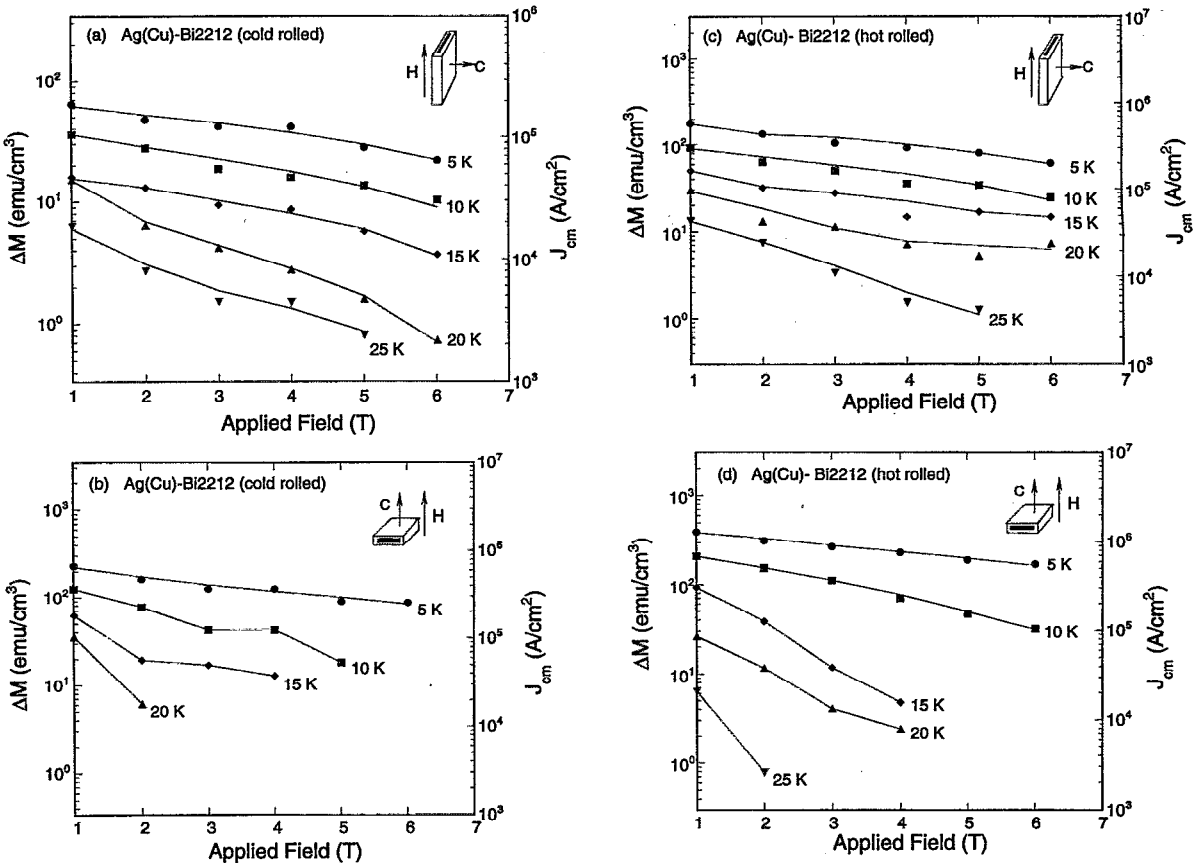

FIG. 11. Plots of magnetization hysteresis width, ΔM, and corresponding magnetization critical current density, J_{cm}, as a function of applied magnetic field for several temperatures for Ag(Cu)-sheathed Bi2212 tapes of varying rolling conditions and sample orientations: (a) cold-rolled ($H\perp c$), (b) cold-rolled ($H\|c$), (c) hot-rolled ($H\perp c$), and (d) hot-rolled ($H\|c$).

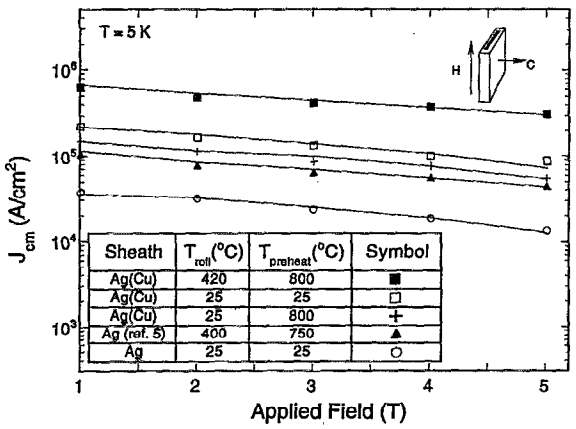

FIG. 12. Comparison of magnetization $J_{cm}(H\perp c)$ as a function of applied field for Ag- and Ag(Cu)-sheathed Bi2212 tapes (Legend indicates roll and preheating furnace temperatures for each sample.)

magnitude lower than the corresponding J_{cm}. Such differences can arise for a number of reasons. For example, magnetooptical imaging results[23,24] suggest that only the superconducting regions closest to the sheath material are effective in carrying current densities approximately equal to the J_{cm} values. Based on this evidence, we attribute the higher J_{ct} values observed for the hot-rolled Ag(Cu)-sheathed tapes at a given applied field and temperature to their enhanced grain alignment and interfacial uniformity.[25]

IV. DISCUSSION

One of the more striking results of this study concerns the microstructural evolution of the Ag(Cu) sheath regions during partial melting of the Bi2212 PIT tapes. Cu_2O (s) precipitates formed rapidly in regions near the outer sheath surface and the sheath/core interface during isothermal heat treatment. These regions grew inward towards the center of the Ag(Cu) sheath (see Figs. 6 and 7), which is indicative of a diffusion-controlled process. At longer times, however, a Cu_2O-deficient zone formed near the sheath/core interface. Excellent agreement was found between this long-term isothermal sheath microstructure and that observed *upon partial* melting of the Ag(Cu)-sheathed Bi2212 tapes. Clearly, the Ag(Cu) sheath is not chemically stable during the thermal processing sequence used for PIT fabrication. A fundamental understanding of these instabilities is necessary to optimize the processing of Bi2212 tapes with alternate sheath compositions because they produce variations in the copper content in the Ag(Cu) solid solution. Such variations influence the mechanical properties of the sheath, as well as the amount of unbound copper available to diffuse from the sheath to the core regions during thermal processing. In this section, we present a theoretical analysis that addresses Cu_2O precipitate formation and, ultimately, the decomposition behavior of this phase in regions near the sheath/oxide core interface at elevated temperatures.

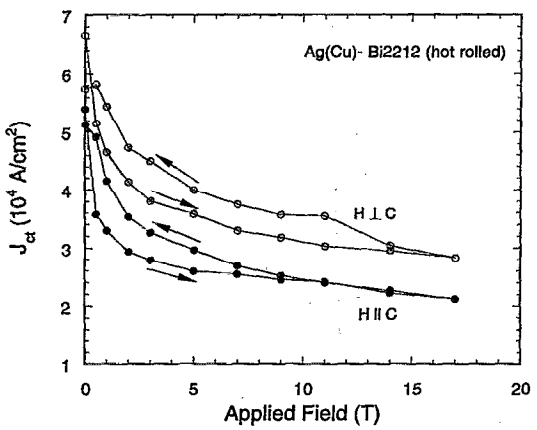

FIG. 13. Plot of transport critical current density, J_{ct}, as a function of applied magnetic field for hot-rolled Ag(Cu)-sheathed Bi2212 tape oriented $H\|c$ and $H\perp c$.

A. Cu_2O formation

Observation of Cu_2O precipitates indicates that the oxidation of copper in the Ag–Cu alloy sheath is energetically favored during partial-melt processing of Bi2212 tapes in air. The amount of copper oxidized from the Ag(Cu) alloy can be estimated from the following expressions. First, considering the reaction equilibrium between $Cu_{(s)}$, $Cu_2O_{(s)}$, and oxygen gas at a given temperature and pressure, one writes:

$$4Cu_{(s)}+O_2=2Cu_2O_{(s)}.$$

The standard free energy change, ΔG^0, for this reaction is given by

$$\Delta G^0=-339{,}000-14.2T\ln T+247T(\text{in joules}) \quad (1)$$

between $T=298$ and 1356 K ($T_{m,Cu}$),[26] and the reaction constant (K) is given by

$$-\ln K=\ln P_{O_2}(eq,T)=\frac{\Delta G^0}{RT}, \quad (2)$$

where R is the gas constant.

Equation (2), which is valid for pure $Cu_{(s)}$ and $Cu_2O_{(s)}$ in their standard states, must be modified to accurately account for the Ag–Cu alloy. In this case, copper with an activity, a_{Cu}, is oxidized from the Ag–Cu solid solution to form $Cu_2O_{(s)}$ at a given temperature, yielding the following expression for the reaction constant

$$-\ln K=\ln[a_{Cu}]^4P_{O_2}(eq,T)=\frac{\Delta G^0}{RT}. \quad (3)$$

Assuming an ideal solution, $a_{Cu}=x_{Cu}=0.07$ (7 at. % Cu), one calculates oxygen partial pressures of 1.25×10^{-4} atm and 9.99×10^{-4} atm at 820 and 885 °C, respectively. The heat treatments, both isothermal and partial melting, were carried out in air (P_{O_2} = 0.21 atm). Under these conditions, one finds from Eq. (3) that 5.91 at. % Cu and 5.18 at. % Cu are oxidized from the Ag–Cu sheath at T_{iso}=820 and 885 °C, respectively. Thus, a small percentage of copper initially present in the sheath region would remain in solid solution at these temperatures.

The kinetics of Cu_2O precipitate formation are governed by the oxygen solubility and its diffusivity in the Ag(Cu) sheath material. Oxygen solubility data for the Ag(7 at. % Cu) alloy are not available. However, the solubility of oxy-

gen in $Ag_{(s)}$ at temperatures between 750 and 950 °C was determined by Ramanarayanan and Rapp[27] using the electrochemical cell method. Under equilibrium conditions, the solubility of oxygen in Ag(s) is given by

$$\begin{aligned} &\tfrac{1}{2}O_2(g, p=1 \text{ atm}) = O(\text{in solid silver}), \\ &\Delta G^0 = 48{,}150 - 16.41T(\text{J/mol}), \\ &K = \frac{[O]}{P_0^{1/2}}, \quad \text{and } \Delta G^0 = -RT \ln K, \\ &[O] = P_0^{1/2} \exp\left(-\frac{\Delta G^0}{RT}\right). \end{aligned} \tag{4}$$

Equation (4) can be used to estimate the oxygen solubility in the sheath region for our heat treatment conditions, for which one calculates oxygen solubilities of 1.65 and 2.22 at. % at $T=820$ and 885 °C, respectively. These respective oxygen solubilities are slightly below those needed to fully oxidize the appropriate amount of copper from solid solution at a given temperature. For example, 2.59 at. % oxygen is needed for 5.18 at. % Cu to be oxidized at 885 °C. Thus, only 4.44 at. % Cu can be oxidized initially, while oxidation of the remaining 0.74 at. % Cu would require additional oxygen transport.

Oxygen diffusivity in the Ag(Cu) sheath regions can be estimated, neglecting oxygen solubility effects, from the width of the Cu_2O precipitate zone (see Figs. 6 and 7) within the Bi2212 PIT tapes, which grows inward from the outer sheath surface and the sheath/core interface during heat treatment. For a one-dimensional geometry, the effective diffusivity is given by

$$d_T^2 = 2D_T t, \tag{5}$$

where d_T is the width of the oxidized zone at a given temperature and time, t. D_T was estimated from Eq. (5) to be 2.22×10^{-8} cm^2/s and 3.53×10^{-8} cm^2/s at 820 and 885 °C, respectively. Widths of the oxidized zones that develop from each interface (i.e., outer surface and sheath/core) are not equivalent. The wider oxidized zone grew inward from the outer-sheath interface, and this value of d_T was used in the above calculations. We have assumed the same initial oxygen partial pressure at both interfaces because the void space between the packed Bi2212 powder within the core regions initially contains air. However, two possible effects that may occur during heat treatment lead to the observed asymmetry in oxidized zone width: (a) oxygen content within the core region becomes depleted, thereby reducing the concentration gradient between the sheath/core interface and the interior sheath region, or (b) Bi2212 decomposition at the sheath/core interface produces a liquid phase that reduces the oxygen transport kinetics. However, our DTA results show that this latter effect would occur only above 858 °C in air.

B. Formation of Cu_2O-deficient zone

In the analysis of Cu_2O formation presented above, diffusion of free copper in Ag(Cu) solid solution from the sheath regions to the oxide core of the PIT tapes was not considered. However, this process occurs concurrently with

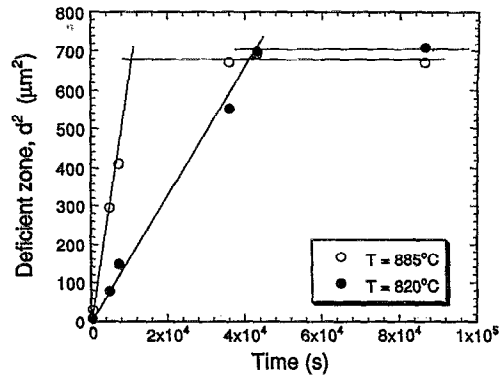

FIG. 14. Plot of squared width of Cu_2O-deficient zone as a function of time for Ag(Cu)-sheathed Bi2212 tapes fired in air at 820 and 885 °C.

Cu_2O precipitate formation during heat treatment and is critical to the long-term development of the Cu_2O-deficient zone near the sheath/oxide interface in the Bi2212 PIT tapes. As copper diffuses from the sheath to the core, the copper activity in the region near the sheath/core interface decreases over time. Based on Eq. (3), as copper activity is reduced in a given region at constant temperature, oxygen partial pressure must be increased to prevent decomposition of the Cu_2O phase. However, because the furnace atmosphere remains the same during heat treatment (i.e., $P_{O_2} = 0.21$ atm), diffusion of copper from the sheath region to the core promotes the local decomposition of Cu_2O precipitates, leading to the observed microstructural development.

The growth of the Cu_2O-deficient zone is governed by copper diffusivity in the Ag(Cu) sheath regions of the Bi2212 PIT tapes at elevated temperatures. Again, assuming a one-dimensional geometry, Eq. (5) can be utilized to estimate an effective copper diffusivity (D_T) based on the observed width (d_T) of the Cu_2O-deficient zone near the sheath/core interface. The width of this zone was measured directly from the SEM photomicrographs shown in Fig. 7. The square of this quantity is shown in Fig. 14 as a function of time for Bi2212 PIT tapes heated isothermally at $T_{iso}=820$ and 885 °C. The width of the Cu_2O-deficient zone initially increases with time and then reaches a plateau value at each temperature. The effective diffusivity of copper in the sheath region is estimated from the short-term data to be 8.1×10^{-11} cm^2/s at 820 °C and 3.1×10^{-10} cm^2/s at 885 °C, respectively. These effective diffusivity values are approximately one order of magnitude lower than the copper diffusivities reported in the literature.[28,29] Furthermore, the effective copper diffusivities are more than two orders of magnitude lower than the effective oxygen diffusivities estimated for the same heat treatment conditions. Such differences provide insight into the competitive rates at which the Cu_2O formation and decomposition processes occur, indicating that these processes can be treated independently, as done in our analysis. The calculated activation energy for the copper diffusion process was found to be 217,289 J/K mol, which yields the following equation for copper diffusivity in the sheath region:

$$D_{Cu}(\text{Ag–Cu}) = 1.96 \exp\left(-\frac{217{,}289\ \text{J}}{RT}\right). \quad (6)$$

A nearly identical plateau value (see Fig. 14) of approximately 25–30 μm was observed for the Cu_2O-deficient zone width upon heat treating the Bi2212 PIT tapes for 12 h at 820 °C and 3.0 h at 885 °C, respectively.

Assuming that the decomposition of Cu_2O is instantaneous and the oxygen concentration is equivalent at both the outer sheath surface and the sheath/core interface during heat treatment, the governing equation and boundary conditions for copper diffusion in the sheath for a one-dimensional geometry are given by

$$\begin{aligned} &\frac{\partial^2 C}{\partial x^2} = \frac{1}{D}\frac{\partial C}{\partial t}, \\ &C = C_0 \quad \text{at } x = 0, \\ &C = C_1 \quad \text{at } x = 70\ \mu\text{m}, \\ &C = C_0 \quad \text{at } t = 0, \quad \text{and } 0 \leqslant x \leqslant 70, \end{aligned} \quad (7)$$

where C_0 and C_1 are the initial free copper concentration at the outer sheath and sheath/core interfaces, respectively, and D is the effective diffusivity of copper in Ag(Cu) alloy, as estimated by Eq. (6). With the Laplace transformation method, the general solution for this expression is given by

$$C = (C_0 - C_1)\sum_{n=0}^{\infty}\left[\text{erfc}\frac{(2n+1)l + x}{2\sqrt{Dt}} - \text{erfc}\frac{(2n+1)l - x}{2\sqrt{Dt}}\right] + C_0. \quad (8)$$

The value for C_1, an unknown quantity in this analysis, is governed by the free copper concentration in the core region of these samples. The calculated concentration profiles of free copper as a function of position (x) for several intermittent times are shown in Figs. 15(a) and 15(b) for T_{iso}=820 and 885 °C, respectively. A value of C_1=0.5 at. % Cu was chosen for these calculations. Each concentration profile was obtained by summing over several terms (n=20) using Eq. (8), for which the relative error is zero. The dashed lines in Fig. 15 illustrate the progressive development of the Cu_2O-free zone of width δx. The final zone thickness was ≈25–30 μm for both isothermal treatments, suggesting that the driving force for copper diffusion from the sheath to the core eventually diminishes.

The isothermal experiments provide insight into the fundamental mass transport processes that occur during heat treatment of Ag(Cu)-sheathed Bi2212 tapes. From the above analysis, we can now determine the progressive microstructural development that occurs during the partial melt processing of these samples. The heat treatment schedule for this process is shown in Fig. 1. Our calculations show that upon completion of the initial hold at 885 °C (t=15 min), the Cu_2O precipitates would exist throughout the sheath regions. However, this amount of time is insufficient to fully establish the Cu_2O-deficient region at this temperature. As the samples are cooled from T_{max}=885 °C to T_{soak}=820 °C, a time period of 13 h elapses for the cooling rate used (i.e.,

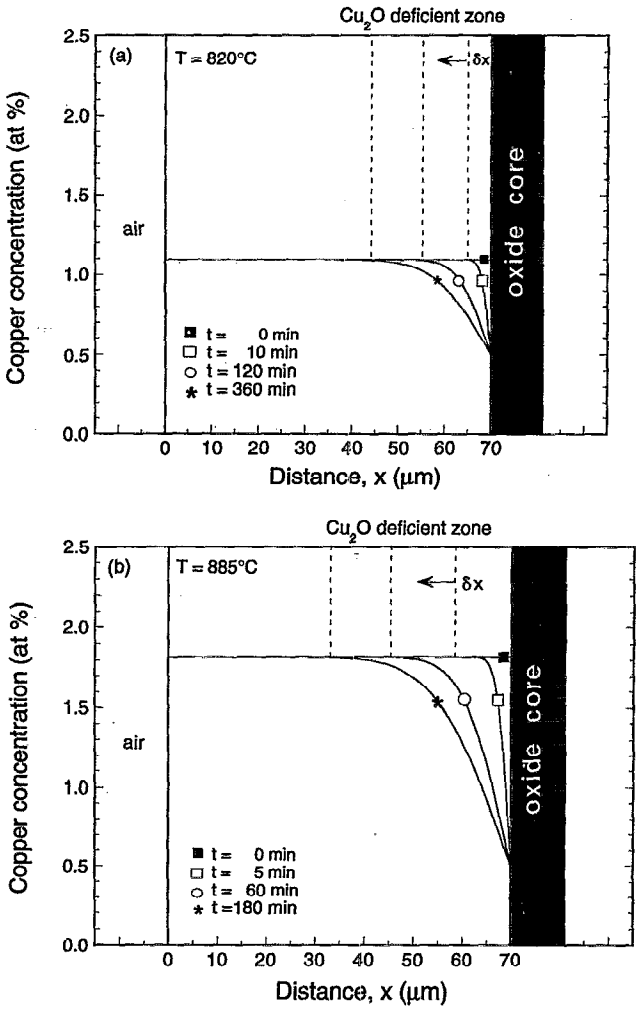

FIG. 15. Calculated concentration profiles of free (or unbound) copper within the sheath region of Ag(Cu)-sheathed Bi2212 tapes at (a) T=820 °C, and (b) T=885 °C. (Arrow indicates the growth direction of the Cu2O-deficient zone.)

5 °C/h). During this temperature transition, the Cu_2O-deficient region should fully develop because only 12 h at 820 °C are actually needed (see Fig. 14) to establish the maximum (or plateau) zone width. Thus, one would not expect further Cu_2O decomposition during the final annealing step at 800 °C for 100 h in air. However, even if the extent of Cu_2O decomposition was minimized during partial melting by reducing the cycle time at elevated temperatures ($T \geqslant 820$ °C), the time necessary to establish a Cu_2O-deficient zone (≈25 μm thick) during the 800 °C annealing step in air is only 17 h, as determined using Eqs. (5) and (6).

Much previous effort has been devoted to optimizing the heat-treatment conditions with respect to T-t parameters and atmospheric conditions to produce high-quality Bi2212 PIT tapes. Thus, it is unlikely that these variables can be dramatically altered to promote chemical stability of the Ag(7 at. % Cu) alloy sheath material. Therefore, we conclude that the dynamic morphological development which occurs during Ag(7 at. % Cu)-sheathed Bi2212 PIT fabrication is unavoidable. An alternative approach to stabilizing the sheath mate-

rial may be to lower the copper content in the alloy to a value that minimizes the formation of the Cu_2O phase. To determine the maximum free copper content allowable, one must examine the thermodynamic and kinetic considerations presented above over the entire temperature range (≈25–885 °C) of the heat-treatment process. One finds that the maximum allowable free copper content decreases significantly with decreasing temperature. While this is coupled with a decrease in oxygen solubility and its effective diffusivity, these parameters are less sensitive to temperature. The maximum tolerable copper content is estimated by our analysis to be $<1.1\times10^{-2}$ at. % Cu for the partial melt processing schedule shown in Fig. 1. Thus, this approach is ineffective because the desired increase in sheath stiffness would be sacrificed at such low copper contents. However, despite the inability to stabilize the Ag(7 at. % Cu) alloy under the current processing conditions, our results demonstrate that significant property improvements can be obtained with these alloys, particularly in conjunction with the hot-rolling process. We attribute these improvements mainly to the hardness difference between the Ag(Cu) and pure silver sheaths (see Fig. 10), which remain present even though this morphological development occurs during the partial-melting process.

The microstructural observations of the Bi2212/Ag(Cu) alloy interactions presented here are in good agreement with earlier work by Nomura *et al.*,[8] as discussed previously. However, our transport measurements sharply contrast those results,[8] which suggested that Ag(Cu) alloys have a deleterious effect on the superconducting properties of Bi2212. For example, Nomura *et al.*[8] reported that J_{ct} values were reduced by more than an order of magnitude at $T=4.2$ K, $H=8$ T for Bi2212 samples heat treated on Ag(2.6 at. % Cu) foil as compared to those processed on pure silver. Several key differences between these experiments prohibit direct comparison, including the starting Bi2212 powder composition, the fabrication process, and heat treatment conditions. In our work, we used a copper-deficient starting powder, $Bi_2Sr_2Ca_{0.64}Cu_{1.64}O_x$, to offset copper absorption between the sheath and core regions. In contrast, stoichiometric $Bi_2Sr_2CaCu_2O_x$ powder was used by Nomura *et al.*,[8] which should exacerbate the formation of the Bi-free phases. Furthermore, we studied cold- and hot-rolled, partially melted and annealed Bi2212 PIT tapes as compared to the doctor blade Bi2212 tapes partially melted on Ag(Cu) alloy (0–2.6 at. % Cu) foils studied by Nomura *et al.*[8] Their observations can be attributed solely to the chemical interactions between stoichiometric Bi2212 and the Ag(Cu) alloys, since further processing was not carried out on their samples after heat treatment. Hence, we offer the following possible explanations for the observed enhancement of transport critical current density, J_{ct}, of the Ag(7 at. % Cu)-sheathed Bi2212 tapes studied here: (1) use of a copper-deficient Bi2212 starting powder minimizes the impact of the deleterious chemical interactions between the sheath and core regions during heat treatment, and (2) enhanced processing of the Ag(Cu)-sheathed Bi2212 tapes at elevated rolling temperatures leads to a net improvement in microstructural development with respect to their current carrying capability.

V. SUMMARY

We have investigated the effects of sheath composition and rolling conditions on the microstructural development and superconducting properties of Bi2212 PIT tapes. The best properties were obtained in hot-rolled, Ag(7 at. % Cu)-sheathed Bi2212 tapes. These samples had the highest degree of grain alignment, improved sheath/core interfacial uniformity, and significantly higher magnetization and transport critical current densities relative to either cold-rolled Ag(Cu)-sheathed or hot- or cold-rolled Ag-sheathed Bi2212 tapes. For example, their transport critical current densities, J_{ct}, at 4.2 K surpassed 2×10^4 A/cm^2 at up to 14 T, with a J_{ct} at zero field of 6.5×10^4 A/cm^2. These values were roughly five times greater than the hot-rolled Ag-sheathed tapes, where $J_{ct}=1.25\times10^4$ A/cm^2 at 4.2 K, 0 T.

A striking feature of our work was the dynamic morphological development in the Ag(Cu) sheath regions of the Bi2212 tapes during their heat treatment, which consisted of partial melting and a final annealing step. Through isothermal studies, we found that Cu_2O precipitates formed uniformly throughout the sheath regions, developing inward from both the outer sheath surface and the sheath/core interface. This was followed by growth of a Cu_2O-deficient zone near the sheath/core interface due to copper diffusion from the sheath to core regions. The loss of free copper from the sheath regions promoted the excess formation of the alkaline-earth cuprate phase within the core regions relative to that formed in the Ag-sheathed Bi2212 tapes. A theoretical analysis of the Cu_2O precipitate formation and decomposition processes suggests that for these heat-treatment conditions, only a negligible amount of free copper can be utilized in the alloy composition to avoid this dynamic morphological development. However, despite the chemical instabilities encountered when utilizing Ag(Cu) alloys as an alternative sheath material for PIT processing of Bi2212 tapes, our results demonstrate that significant property improvements can be obtained with these alloys, particularly in conjunction with a hot-rolling process. We have attributed these observations to the hardness differences between the Ag(Cu) and pure Ag sheath materials that persist in spite of these instabilities. Our work highlights the need to investigate other alloy compositions (e.g., Ag–Al or Ag–Mg alloys) that may provide similar property improvements to those demonstrated by this study, but that avoid the deleterious attributes of the Ag(Cu) alloy system.

ACKNOWLEDGMENTS

This work was supported by the U.S. Department of Energy (DOE), Energy Efficiency and Renewable Energy, as part of a DOE program to develop electric power technology, and Basic Energy Sciences-Materials Sciences, under Contract No. W-31-109-Eng-38. The authors thank Y. Tanaka and H. Maeda for supplying the Ag(Cu)-sheathed Bi2212 samples, Y. Hascicek and J. Kessler for carrying out high-field transport measurements, and Markus Wegmann for several fruitful discussions of this work.

[1] H. Sekine, J. Schwartz, T. Kuroda, K. Inoue, H. Maeda, K. Numata, and H. Yamamoto, J. Appl. Phys. **70**, 1596 (1991).
[2] C.-T. Wu, K. C. Goretta, and R. B. Poeppel, Appl. Supercond. **1**, 33 (1993).
[3] P. Haldar, J. G. Hoehn, Jr., J. A. Rice, and L. R. Motowidlo, Appl. Phys. Lett. **60**, 495 (1992).
[4] W. Gao and J. B. Vander Sande, Supercond. Sci. Technol. **5**, 318 (1992).
[5] J. Guo, J. Schwartz, Y. S. Cha, C.-T. Wu, and K. C. Goretta, Adv. Cryog. Eng. **40**, 169 (1994).
[6] J. Guo, J. Schwartz, C.-T. Wu, and K. C. Goretta, IEEE Trans. Magn. **30**, 2098 (1994).
[7] A. Perin, G. Grasso, M. Däumling, B. Hensel, E. Walker, and R. Flükiger, Physica C **3-4**, 339 (1993).
[8] K. Nomura, T. Sasaoka, J. Sato, and S. Kuma, H. Kumakura, K. Togano, and N. Tomita, Appl. Phys. Lett. **64**, 112 (1994).
[9] C. P. Bean, Phys. Rev. Lett. **8**, 250 (1962).
[10] K. Heine, J. Tenbrink, and Thöner, Appl. Phys. Lett. **55**, 2441 (1989).
[11] D. R. Dietderich, B. Ullmann, H. C. Freyhardt, J. Kase, H. Kumakura, K. Togano, and H. Maeda, Jpn. J. Appl. Phys. **29**, L1100 (1990).
[12] J. Schwartz, H. Sekine, T. Asano, T. Kuroda, K. Inoue, and H. Maeda, IEEE Trans. Magn. **27**, 1247 (1991).
[13] H. Kumakura, K. Togano, D. R. Dietderich, H. Maeda, J. Kase, and T. Morimoto, IEEE Trans. Magn. **27**, 1250 (1991).
[14] K. C. Goretta and D. Shi, Appl. Phys. Commun. **11**, 317 (1992).
[15] K. H. Sandhage, G. N. Riley, Jr., and W. L. Carter, J. Met. **43**, 21 (1991).
[16] S. Jin and J. E. Graebner, Mater. Sci. Eng. B **7**, 243 (1991).
[17] I. Bloom, J. R. Frommelt, M. C. Hash, M. T. Lanagan, C.-T. Wu, and K. C. Goretta, Mater. Res. Bull. **26**, 1269 (1991).
[18] Y. F. Li, M. E. Loomans, K. C. Goretta, S. E. Dorris, M. T. Lanagan, R. B. Poeppel, J. J. Wenzlaff, P. M. Winandy, C. A. Youngdahl, and U. Balachandran, J. Electron. Mater. **23**, 1163 (1994).
[19] S. Wu, J. Schwartz, J. C. Rynes, and C. A. Gianino, Appl. Supercond. **1**, 93 (1993).
[20] J. Schwartz and S. Wu, Physica C **190**, 169 (1991).
[21] J. Schwartz and S. Wu, Physica C **185-189**, 2403 (1991).
[22] J. Guo, J. A. Lewis, J. Schwartz, and K. Goretta, IEEE Trans. Appl. Supercond. **5**, 1860 (1995).
[23] D. Larbalestier, X. Y. Cai, H. Edelman, M. B. Field, J. Parrell, A. Pashitski, and A. Polyanskii, J. Met. **46**, 20 (1994).
[24] A. E. Pashitski, A. Polyanskii, A. Gurevich, J. Parrell, and D. Larbalestier Physica C (submitted).
[25] R. H. Arendt, M. F. Garbauskas, K. W. Lay, and J. E. Tkaczyk, Physica C **194**, 383 (1992).
[26] D. R. Gaskell, *Introduction to Metallurgical Thermodynamics*, 2nd Ed. (Hemisphere, New York, 1981).
[27] T. A. Ramanarayanan and R. A. Rapp, Met. Trans. **3**, 3239 (1972).
[28] J. R. Cahoon and W. V. Youdelis, Trans. Metall. Soc. AIME **29**, 127 (1967).
[29] A. Sawatzky and F. E. Jaumot, Jr. J. Met. **9**, 1207 (1957).